International Journal of Fluid Machinery and Systems
Vol. 3, No. 1, January-March 2010

Original Paper

Flow Investigations in the Crossover System of a Centrifugal Compressor Stage

K. Srinivasa Reddy[1], G. V. Ramana Murty[2], A Dasgupta[3] and K. V. Sharma[4]

[1] Department of Mechanical Engineering, Aurora's Engineering College
Bhongir, 508116, India
[2] Department of Mechanical Engineering, Vasavi College of Engineering
Hyderabad, India
[3] Turbomachinery Laboratory, Corporate R&D Division
Bharat Heavy Electricals Limited, Hyderabad, 500093, India
[4] Faculty of Mechanical Engineering, Universiti Malaysia Pahang
26600, Pekan, Pahang, Malaysia

Abstract

The performance of the crossover system of a centrifugal compressor stage consisting of static components of 180^0 U-bend, return channel vanes and exit ducting with a 90^0 bend is investigated. This study is confined to the assessment of performance of the crossover system by varying the shape of the return channel vanes. For this purpose two different types of Return Channel Vanes (*RCV1* and *RCV2*) were experimentally investigated. The performance of the crossover system is discussed in terms of total pressure loss coefficient, static pressure recovery coefficient and vane surface pressure distribution. The experimentation was carried out on a test setup in which static swirl vanes were used to simulate the flow at the exit of an actual centrifugal compressor impeller with a design flow coefficient of 0.053. The swirl vanes are connected to a mechanism with which the flow angle at the inlet of U-bend could be altered. The measurements were taken at five different operating conditions varying from 70% to 120% of design flow rate. On an overall assessment *RCV1* is found to give better performance in comparison to *RCV2* for different U-bend inlet flow angles. The performance of *RCV2* was verified using numerical studies with the help of a CFD Code. Three dimensional sector models were used for simulating the flow through the crossover system. The turbulence was predicted with standard k-ε, 2-equation model. The iso-Mach contour plots on different planes and development of secondary flows were visualized through this study.

Keywords: Centrifugal Compressor, Return Channel Vanes, Inlet Flow Angle, Swirl Angle, Performance, Vane Surface Pressure Coefficient

1. Introduction

The aerodynamic performance of 180^0 U-bend, return channel vanes and exit ducting which form the crossover system, influences the overall performance of the stage of a centrifugal compressor. The performance optimization of these individual components is crucial in reducing the power consumption requirements of centrifugal compressors. The flow coming out of the centrifugal compressor impeller is having significant tangential velocity component as it enters the crossover 180^0 circumferential bend. The swirling flow is subjected to sharp curvature in the 180^0 U-bend resulting in intense energy exchanges before it enters the return channel vanes. In return channel vanes the flow is further decelerated in the process of removing the swirl. This deceleration of flow which has significant tangential component of velocity leads to the development of cross flows. Simon and Rothstein [1] created a test bed for carrying out systematic measurements on return channel passages with three different geometries of return channel vanes. They reported about the nature of flow taking place through the return channel vanes and emphasized the need to describe the flow with the aid of simplified calculation models. In a similar fashion Inoue and Koizumi [2] conducted experimental investigations on an entire flow model for return passages including a U-turn bend, deswirl vane section and an L-turn section at the exit. They reported the presence of secondary flow in U-turn and exit L-turn sections.

Received June 24 2009; revised September 25 2009; accepted for publication October 26 2009: Review conducted by Dr. Hideaki Tamaki. (Paper number O09022)
Corresponding author: K. Srinivasa Reddy, kommareddy_s@yahoo.com

Because of the secondary flow in deswirl vanes, the flow has a swirl component at the return channel exit. They also concluded that most of the losses in deswirl vane section can be attributed to the flow separation for small inlet flow angle. Lenke and Simon [3] conducted CFD studies and showed that for small flow coefficient flows, the frictional losses are more dominant and increase the loss coefficients whereas for higher flow coefficients secondary flow increases and care has to be taken to avoid small streamline radius of curvature within the crossover bend. Veress and Braembussche [4] presented the inverse design and optimization of a multistage radial compressor stage consisting of a vaneless diffuser, crossover bend and return channel. They studied the impact of vane lean on secondary flows and showed performance improvements with negative lean. A numerical study of the U-turn bend in return channel systems for multistage centrifugal compressors was conducted by Oh et. al [5]. They have discussed in detail the loss mechanisms in the U-turn bend along with the effect of turbulence models on the flow behaviour. Toshiaki Kanemoto and Tomitaro Toyokura [6] designed a circular cascade for a return channel of a centrifugal turbo machine, whose vane height varies in the radial direction using singularity method. They also developed a circular cascade model and tested its performance experimentally [7]. They concluded that the minimum flow loss is given at a small positive incidence angle and the mixing loss downstream of the cascade is considerable. In the present study an experimental test rig was developed with static swirl vanes to simulate the flow through an actual impeller of a centrifugal compressor to study the performance of return channel vanes with two different geometries namely *RCV1* and *RCV2*. *RCV2* is evolved from *RCV1* by increasing the blade chord and blade thickness by 8.0% and 12.5% respectively with an alteration in the inlet blade angle. A commercial flow solver, FLUENT was used to assess the performance of the return channel vane geometry, *RCV2* expecting the performance to improve. The results are discussed in the following sections.

2. Test Setup

A test-bed for conducting experimental investigations in the crossover system of a centrifugal compressor stage was developed. The flow through the actual centrifugal compressor impeller passage is simulated by passing it through a set of static swirl vanes. As reported in the literature [1], the fundamental character of the flow at the exit of a swirl vane unit differs from that of the impeller exit in that the impeller displays an unsteady discharge flow with the mixing of wakes, where as the flow after a fixed swirl vane unit is characterized by quasi-stationary wakes. The comparison of the two forms of flow is justified approximately at inlet of the crossover bend, but probably better at the exit of 180^0 bend because of intensive energy exchanges taking place in parallel walled vaneless diffuser and circumferential U-bend. Figure 1 shows the sectional view of the test setup in the meridional plane. The flow path width at various locations of the geometry, applicable for both the configurations *RCV1* and *RCV2* is expressed in non-dimensional form as shown in Table 2.1. The design flow angles for *RCV1*and *RCV2* are shown in Table 2.2. The actual width is divided with a known constant, *K*. The air is drawn in from atmosphere by a blower, delivering a design flow rate of $2.5 m^3$/sec, imparting a head of 440 mm of water column at 1500rpm driven by an induction motor of capacity 50 kW. Downstream of the swirl vanes, the flow enters a parallel walled vaneless passage to simulate the vaneless diffuser. The flow then enters 180° U-turn bend which has a straight portion towards the exit which is an existing design feature. The radius ratio of diffuser, U-bend and return channel vane configuration is simulated corresponding to an impeller flow coefficient of 0.053 (a ratio of volume flow rate passing through the impeller to the product of tip speed and area at the exit of impeller). From the 90^0 bend exit, the air enters an annular passage followed by a cone, straight duct before entering a venturi nozzle for measurement of flow rate. A straight duct of diameter 500 mm carries the flow out of the venturi nozzle into the atmosphere. The mass flow rate through the test section is varied by varying the speed of the blower. The required flow angle at U-bend inlet is obtained by rotating the swirl vanes about a point passing through its camber line with the help of linkage mechanism. This mechanism helps in varying the flow angle at U-bend inlet over a wide range.

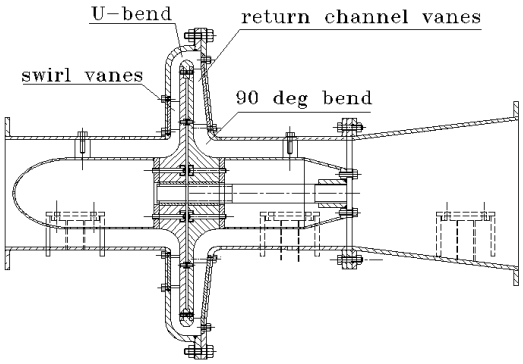

Fig. 1 Sectional view of the test setup

Table 2.1 Channel widths at various locations		
Location	Channel width (b/K)	Radius Ratio (r/r_L)
1. U-bend inlet	0.049	0.947
2. U-bend exit	0.041	1.021
3. *RCV* exit	0.078	0.556
4. L-turn exit	0.095	---

Table.2.2 Design flow angles for *RCV1* and *RCV2*		
Parameter	*RCV1*	*RCV2*
Vane inlet angle	28.5^0	27^0
Vane exit angle	82^0	82^0

3. Measurement Locations and Instrumentation

The reference static pressure from the settling chamber located at the upstream of test setup and wall static pressures at the required locations were measured from the wall tappings provided at these locations. The settling chamber temperature was measured with a Platinum resistance temperature sensor with a digital display having a least count of 0.1°C. A three-hole wedge probe with a head diameter of 3 mm was used at U-bend inlet (Location 1), U-bend exit (Location 2) and exit ducting (Location 4), as shown in Fig. 2(a), for flow field measurement. The pressures at different locations were measured using a micromanometer

along with a multi-channel selector box with a least count of 0.1mm water column. The instrumentation used for flow field measurement was calibrated before the start of experiment. The static pressure distribution at the mid span of return channel vane was obtained using hypodermic tubing embedded on the vane surface with a hole diameter of 1mm. This data was collected at 34 locations on the suction and pressure surface of the vane from leading edge to trailing edge. The venturi nozzle was calibrated to estimate the flow rate at various speeds. The reference speeds have been chosen so that various flow conditions were covered above and below that of design mass flow rate. The flow field is traversed from hub to shroud at three locations as shown in Fig.2 (a). The probe was traversed from hub to casing at one station of location 1, where as circumferential traversing was carried out at 11 stations and 9 stations respectively of Location 2 and 4. Figure 2(b), shows the photograph of measuring stations at U-bend exit.

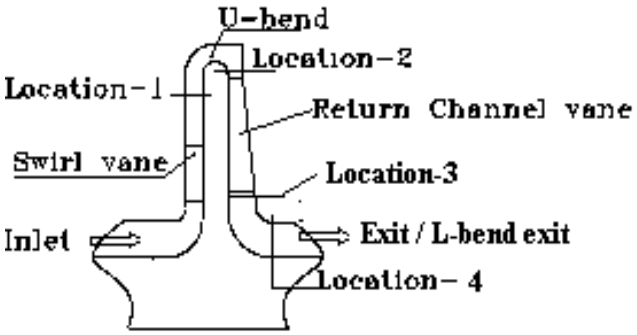

Fig. 2(a) Measuring locations in the meridional plane

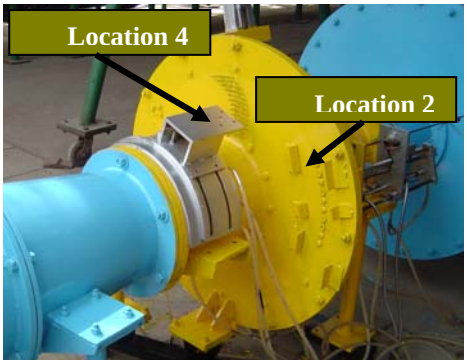

Fig. 2(b) View showing the test setup

4. Experimental Results and Discussion

The experimental flow investigations on *RCV1* and *RCV2* were conducted by maintaining the average absolute flow angles of 21°, 24°, 29°, 32° and 34° at the vaneless diffuser exit, corresponding to design flow rate of 70%, 80%, 100%, 110% and 120% respectively. The design point average absolute flow angle at vaneless diffuser exit corresponding to its flow rate is 29° [8], with respect to tangential direction. The absolute flow angle at the exit of diffuser increases/decreases with increase/decrease in flow rate and the corresponding values were set in the experiment. The required flow rate is achieved by changing the speed of the blower and the flow angle is set by adjusting the swirl vane variable angle mechanism. Once the flow conditions are established, the measurements were taken using the wedge probe at different locations mentioned earlier. The results are presented in non-dimensional form wherever applicable showing the variation of meridional velocity, flow angle, return channel vane surface pressure distribution and exit swirl angle distribution in the following sections. The overall performance of the static components is discussed in the form of variation of total pressure loss coefficient and static pressure recovery coefficient with respect to the U-bend inlet flow angle.

4.1 Meridional Velocity and Flow Angle Distribution in 180^0 U-bend

The design point meridional velocity distribution and the corresponding absolute flow angle distribution at the inlet of 180^0 U-bend for chosen return channel geometries (*RCV1* and *RCV2*) are shown in Fig. 3. The nature of variation for both the vane configurations remains unaltered. The meridional velocity is more concentrated towards the hub with the peak value occurring at about a non-dimensional distance of 0.7 from shroud. This variation is generally in agreement with the results shown by Inoue and Koizumi [2] who have carried out experiments using similar setup having static swirl vanes and their observations are in line with the present study and thus can be considered as typical for such test configuration. This variation suggests the presence of strong swirl at the inlet of U-bend resulting in non-uniform mass flow distribution along the width of the flow path. The presence of return channel vanes seems to have an effect on the non-uniform flow angle distribution in the upstream section of U-bend inlet. The flow angle is observed to increase up to certain distance from shroud and the magnitude of flow angle is seen to dip towards the hub. Lower absolute flow angles are observed for *RCV2* in comparison to *RCV1* up to a non-dimensional distance of 0.7 from shroud and there after higher absolute flow angles are observed towards the hub.

The variation of circumferentially averaged meridional velocity and the corresponding flow angle distribution at the exit of 180^0 U-turn bend is shown in Fig. 4. The meridional velocity for *RCV1* is seen to be nearly uniform from hub to shroud while there is a monotonic decrease of meridional component of velocity from shroud to hub for *RCV2*. The shape of the return channel vane appears to have an effect on the incoming flow at the *L.E* of return channel vane. Further the swirl component appears to have smoothened out at the exit of U-bend in comparison to inlet. The average flow angle is observed to decrease towards the hub for both the configurations. The main flow is directed towards the shroud while the inner flow is reduced due to sharp turning. The flow angles are measured with respect to tangential direction at U-bend inlet and exit. The flow enters the U-bend with a tangential swirl and undergoes sharp 180^0 turning before it enters the return channel vanes. The increase in the average flow angle from Location 1 to Location 2 is due to the decrease in passage width by about 16% which results in the increase of meridional component of velocity for satisfying the continuity equation. The measured average flow angles at U-bend exit are observed to be approximately 4^0 higher in magnitude than at the U-bend inlet.

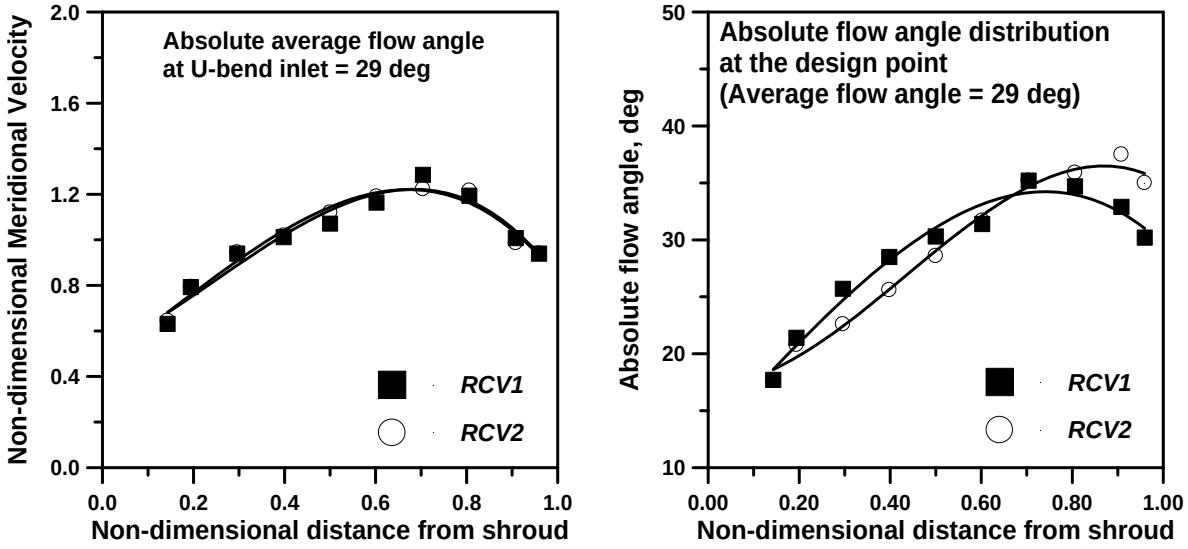

Fig. 3 Variation of meridional velocity and absolute flow angle at 180^0 U-bend inlet

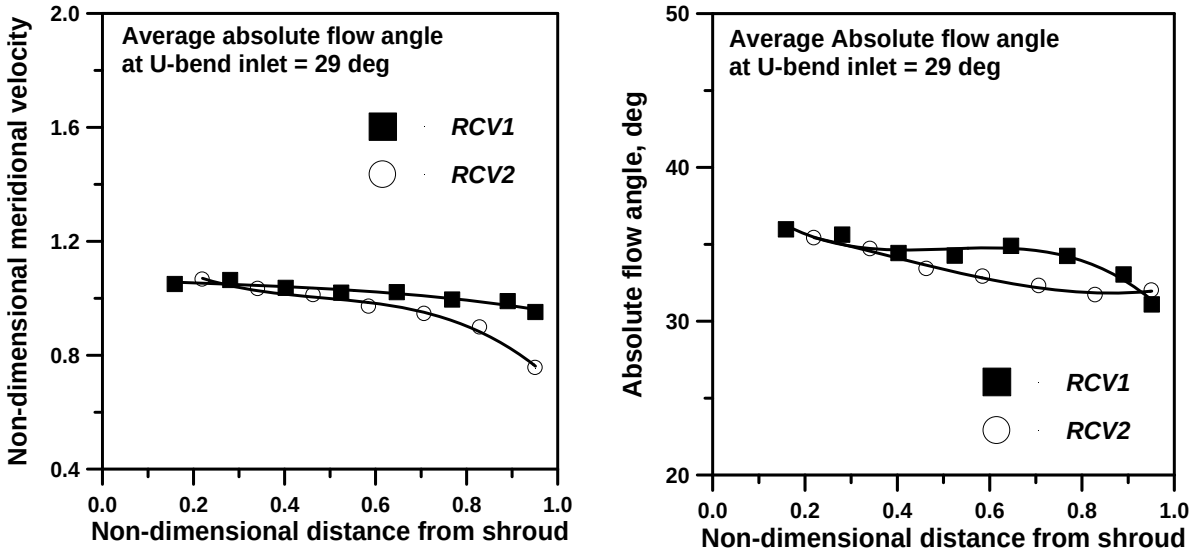

Fig. 4 Variation of meridional velocity and absolute flow angle at 180^0 U-bend exit

4.2 Vane Surface Pressure Distribution

The static pressures measured on the return channel vane surface for both the configurations were expressed as vane surface pressure coefficient (C_{pv}). The C_{pv} values plotted against the percentage chord length from the *L.E* at the design point is shown in Fig. 5. The surface pressure distribution is seen to have a change on the pressure and suction surface for the two tested configurations. The loading pattern for *RCV1* and *RCV2* is the same on pressure side (PS) of the vane from 50% to 100% of the chord length. Similarly on the suction side (SS) of the vane the loading is similar from 70% to 100% of the chord length for both the configurations. A significant difference in the loading on PS is observed up to 50% of the chord length for the two return channel geometries. *RCV1* appears to be more uniformly loaded on the PS as compared to *RCV2*. On the PS of *RCV2*, a sudden drop in static pressure from positive to negative values and there after recovering again to positive values is observed, indicating possible flow separation and reattachment on the PS towards the leading edge. The vane loading patterns as observed from Fig. 5 indicates higher losses due to flow separation for *RCV2* as compared to *RCV1* configuration.

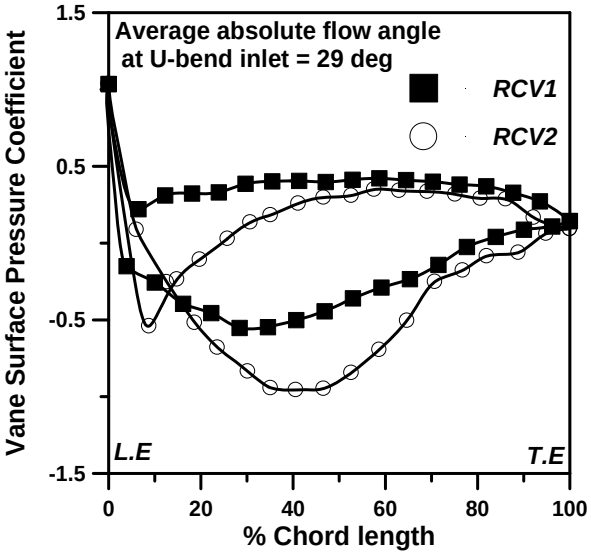

Fig. 5 Vane surface pressure distribution

4.3 Meridional Velocity and Swirl Angle Distribution at the Final Exit

The non-dimensional meridional velocity and swirl angle distribution from shroud to hub at three circumferential locations of stage exit corresponding to -20^0, 0^0 and $+20^0$ for $\alpha_1 = 29^0$ are shown in Fig. 6. The 0^0 position corresponds to vertical traverse at this plane which coincides with the trailing edge of the vane. The angular pitch of the vanes is 20^0 and as such the circumferential traverse covered two vane pitches. The meridional velocity is observed to increase from shroud to hub for both the configurations and the magnitudes are almost same at -20^0 and 0^0 circumferential locations. At $+ 20^0$ circumferential location, the meridional velocity for *RCV2* is seen to be higher than *RCV1* from shroud to 80% of the flow width. The magnitude of meridional velocity is more towards the hub, suggesting that the flow on turning is moved away from shroud. The exit swirl angle for *RCV1* is seen to be varying between 93^0 and 100^0, measured with respect to tangential direction. The swirl angle for *RCV2* is observed to be smaller near the hub as well as shroud, while it is found to be higher between non-dimensional distances of 0.3 to 0.7 from shroud. Due to the curvature of the vane there is a possibility of flow getting separated on the suction side, towards the trailing edge, particularly with positive incidence on return channel vane leading edge. As the flow enters the inlet of 90^0 bend immediately after the exit from return channel vanes, it is subjected to development of secondary flows from PS to SS. These secondary flows cause not only increase in fluid friction losses but also the exit swirl to increase. The magnitude of swirl angle distribution for *RCV1* is observed to be higher than *RCV2*, indicating more turning with *RCV2*. This may be due to the predominant secondary flows in the mid region of the flow path width in the exit ducting. The magnitude range of swirl angle variation is observed to be almost same for both the channels.

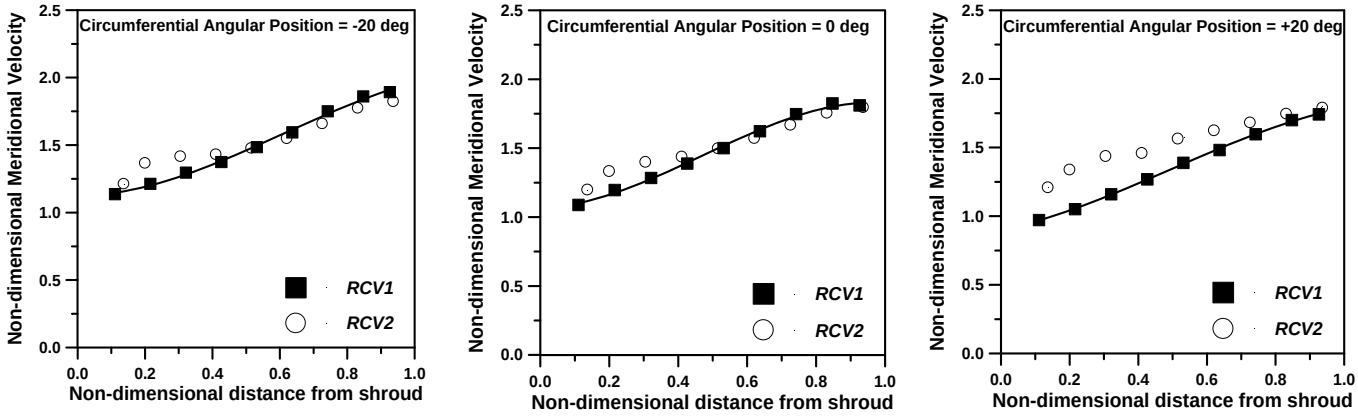

(a) Meridional velocity at stage exit

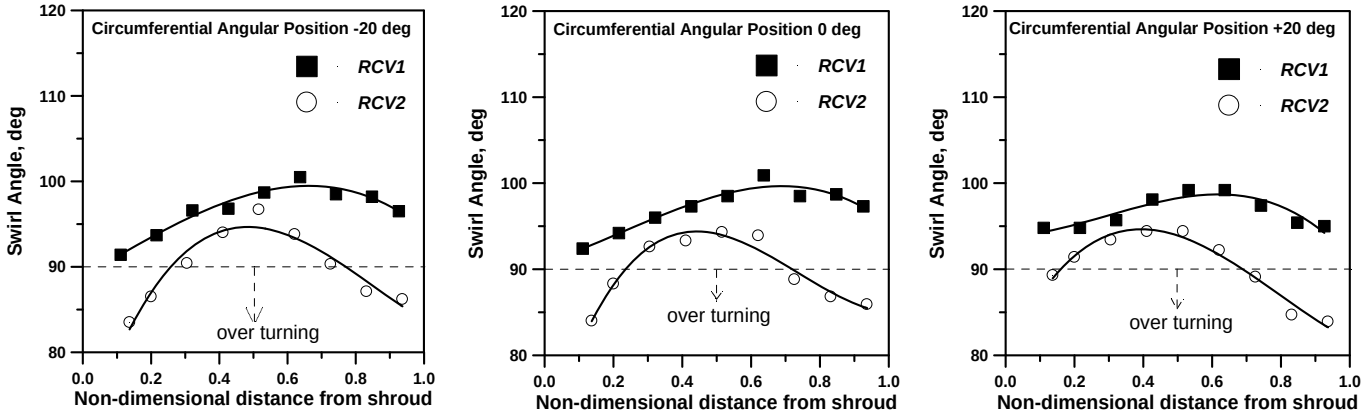

(b) Swirl angle at stage exit

Fig. 6 Variation of meridional velocity and swirl angle at stage exit ($\alpha_1 = 29^0$)

5. Performance Comparison

The performance comparison for *RCV1* and *RCV2* is carried out in terms of total pressure loss coefficient and static pressure recovery coefficient for the stage. The variation of these coefficients with absolute flow angle at U-bend inlet for the chosen configurations is shown in Fig. 7(a) and 7(b) respectively. The total pressure loss coefficient (ζ) is observed to increase with increase in absolute flow angle at U-bend inlet for both *RCV1* and *RCV2*, though the rate of increase is faster for *RCV2* configuration. It may also be seen that the performance is nearly identical at 21^0 U-bend inlet flow angle. As a whole the total pressure loss behavior of *RCV1* appears to be better than *RCV2* over the tested U-bend inlet flow angle range. The static pressure recovery coefficient (C_p) for *RCV1* and *RCV2* is seen to decrease with increase in the U-bend inlet flow angle. There is no

pressure recovery beyond 30^0 of U-bend inlet absolute flow angle. The pressure recovery is observed to be higher over the tested range for *RCV1* than *RCV2*. Based on these two coefficients, it may be concluded that the *RCV2* configuration performance is inferior to *RCV1*. The same was verified using computational techniques and the results of *RCV2* configuration are discussed in the next section.

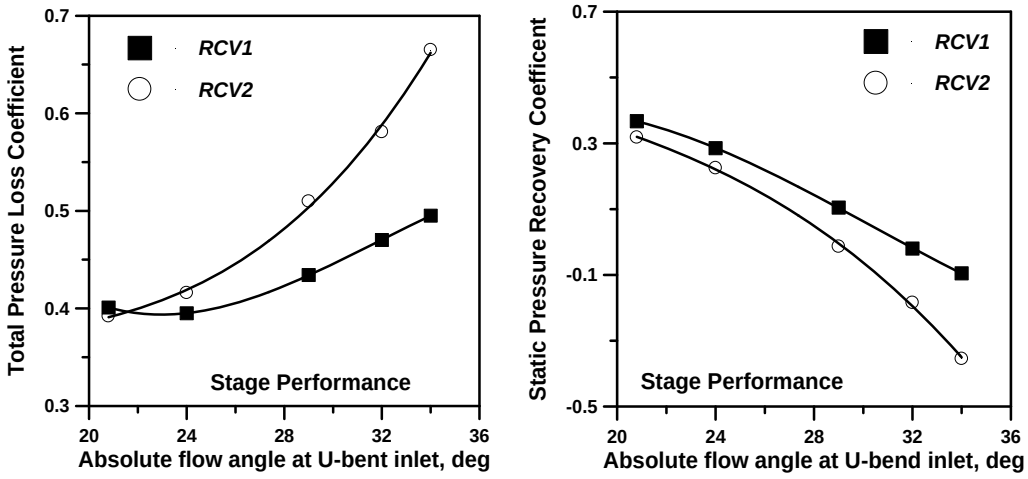

(a) Total pressure loss coefficient (ζ_4) (b) Static pressure recovery coefficient (C_{p4})

Fig. 7 Variation of aerodynamic performance parameters for the stage

6. Numerical Studies

6.1 Modelling of Flow Geometry

The three dimensional sector models are considered appropriate for this analysis as the flow passages are axi-symmetric. This procedure also minimised the computer memory requirement and allowed grid refinement in critical regions [9]. Structured hexahedral 3D elements are used for U-bend and exit 90^0 bend sections while unstructured hex/wedge elements are used for the grid setup in return channel vanes. The total grid size consists of 2, 51,460 hexahedral cell volumes. The computational mesh used for U-bend, L-turn exit and *RCV2* are shown in Fig. 8. The exit section of 180^0 U-bend and inlet section of return channel vanes are coupled with "interface" feature available in the program. Similarly the exit section of return channel vanes and inlet section of 90^0 bend are coupled with interface feature. Near the walls of flow geometry the grid is refined. To capture the flow separation, fine grid features were used on the return channel vane surface and wall surfaces. At the inlet section, the fluid properties and the total pressure along with flow angle were specified. The data obtained from experimental investigations were specified as inlet boundary conditions in the present study for ease of comparison. At the exit section of 90^0 bend, the static pressure with radial equilibrium pressure distribution option with target mass flow rate was used as outlet boundary condition. To ensure that the solution is obtained with sufficient grid spacing for accuracy, grid sensitivity studies were conducted with different interval spacing. The total pressure loss coefficient is chosen as the basic parameter to decide the optimal grid size. Based on the study, the solution was found to be grid independent with an interval size of 0.002 meters. Thereafter all the solution runs were conducted at this grid size for the chosen geometry. The pressure based solver with implicit formulation under 3D steady flow conditions with absolute velocity formulation is chosen. In the present study the standard k–ε model is used to predict the turbulence as it was reported in the literature that Oh et.al, [5] conducted similar studies and predicted the turbulence closer to the experimental observations using the same model. The near wall treatment is handled with standard wall functions. The second order upwind scheme is used for discretization of convection terms. The solution was obtained with the maximum residual values equal to 1e-06.

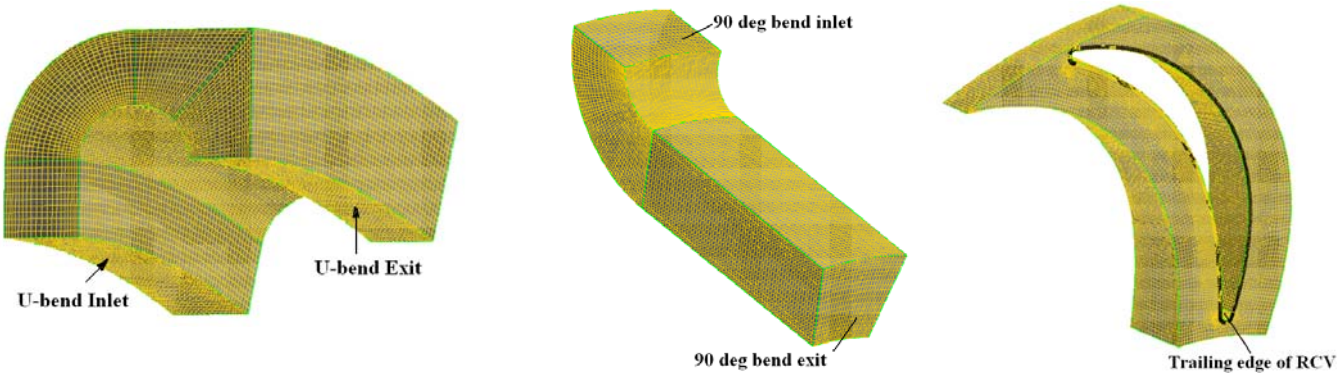

Fig. 8 Computational mesh for U- bend, 90^0 bend and *RCV2*

6.2 Results and Discussion

The fluid flow simulation in the computational domain was carried out for the five different operating conditions corresponding to 120%, 110%, 100%, 80% and 70% of design flow rate exactly similar to the values used for the experiments. After post processing, the results are presented in the form of iso contours of Mach number in the return channel passage as well on the vane surface. For reasons of brevity, the results corresponding to 100% flow rate, at an average U-bend inlet absolute flow angle of 29^0 are shown in Figs. 9 to 11. Figure 9 shows the Iso-Mach number contour plots on different planes along the flow path. Plane 1 corresponds to radius ratio (ratio of radius at which the plane is selected to the radius at which *L.E* is placed) of 0.99, which is very near to the leading edge. The iso-contours of Mach number at this plane indicate acceleration of flow towards the suction surface of the vane. Deceleration is seen to occur at Plane 2 which corresponds to a radius ratio of 0.9, as the flow progresses within the vane passage from Plane 1. Considerable pressure gradient has been observed at Plane 3 (radius ratio of 0.7) from SS to PS. Regions of low flow is seen to occur at plane 3 near the suction surface represented by iso-Mach contours of low magnitude. The iso-contour plot at the trailing edge upstream region of the vane is shown in Plane 4, which is at a radius ratio of 0.52. It is observed that near the SS the low flow regions are widened as represented by iso-Mach contours of low magnitude. The flow at the downstream region of the vane is represented in Plane 5 (inlet of 90^0 bend). The region of flow separation is clearly seen on the SS of plane 5. The region of flow separation is indicated by the low magnitude of Mach number. The flow is seen to be concentrated towards the shroud at this plane. The spread of the low velocity region at inlet to 90^0 bend is seen on this plane. Figure 10 shows the calculated secondary flows on plane 5 of *RCV1* and *RCV2*. The secondary flow pattern on plane 5 suggests relatively more turning for *RCV2* than *RCV1*. Figure 11 shows the iso-Mach contours on a plane through the mid span of the flow channel width in which the low Mach number contours are clearly seen on the downstream of suction side of the vane. This low velocity region is spreading into the inlet of the 90^0 bend as also can be seen on plane 5 of Fig. 9. It may be noted that the low velocity region which is spreading from the trailing edge of the vane into the 90^0 bend might be inducing some cross flow from PS to SS.

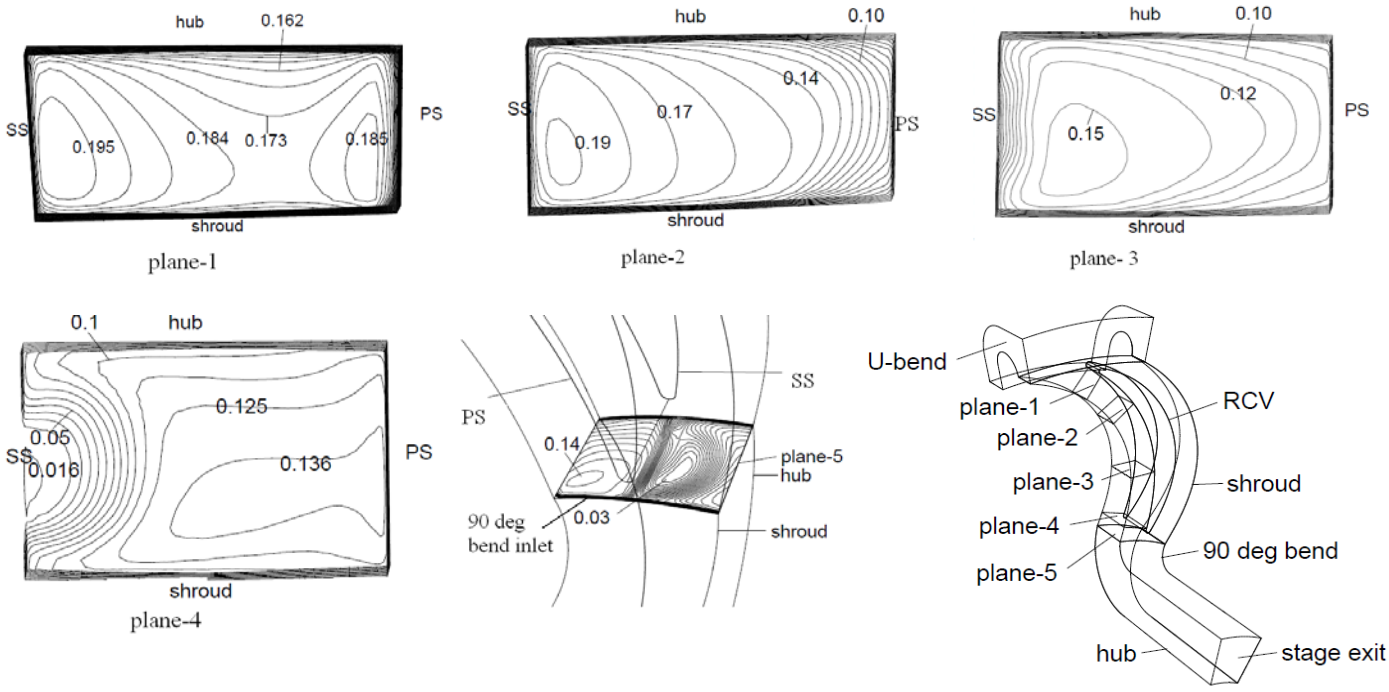

Fig. 9 Calculated iso-contours of Mach number along the flow path (*RCV2*) (α_1= 29^0)

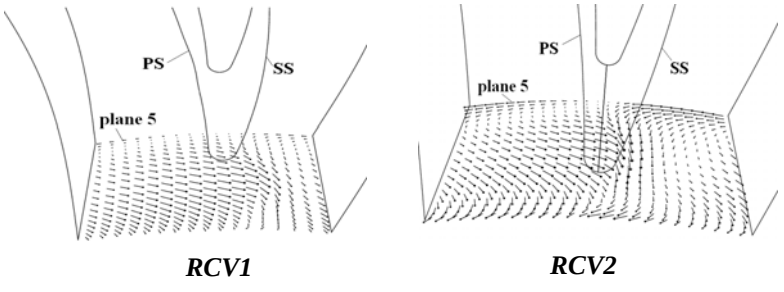

Fig. 10 Calculated cross flow velocity vector plot for *RCV1* and *RCV2* (α_1 = 29^0)

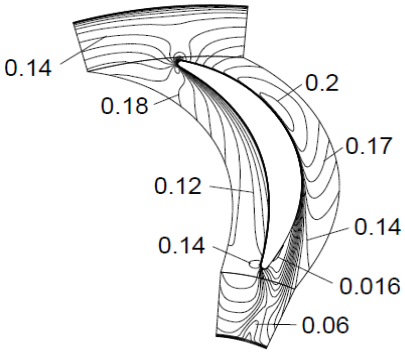

Fig. 11 Iso-contours of Mach number around the return channel vane at mid span (*RCV2*) (α_1 = 29^0)

7. Comparison of Results

Figure 12 shows the comparison of experimental and CFD results at various locations in respect of meridional velocity, absolute flow angle, total pressure loss coefficient, static pressure recovery coefficient, circumferentially averaged swirl angle at stage exit and vane surface pressure coefficient. These parameters represent the overall performance of the return channel vane system. The CFD results display a near agreement with the experimental observations. It may be concluded from the present study that the *RCV2* configuration is contributing to increased losses in the flow channel due to flow separation near the leading edge as the U-bend inlet flow angle is increased. Figure 13 shows the performance of U-bend in terms of total pressure loss coefficient and static pressure recovery coefficient for *RCV2*. There is no static pressure recovery in the U-bend and negative recovery is observed with increase in U-bend inlet flow angle. The minimum total pressure loss coefficient is observed at a U-bend inlet flow angle of 27^0. The total pressure loss coefficient is seen to increase symmetrically on either side of 27^0.

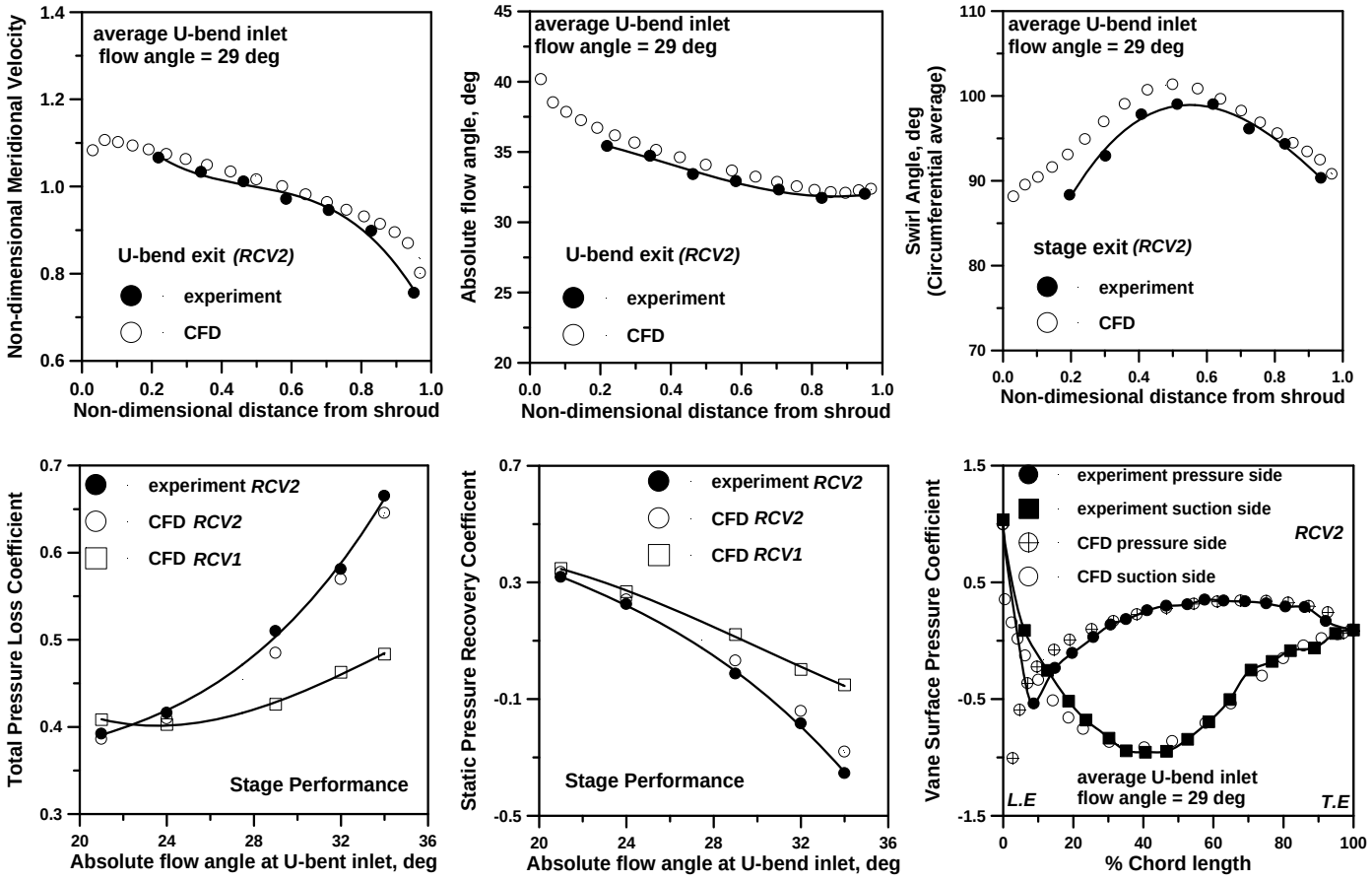

Fig. 12 Comparison of experimental and numerical data

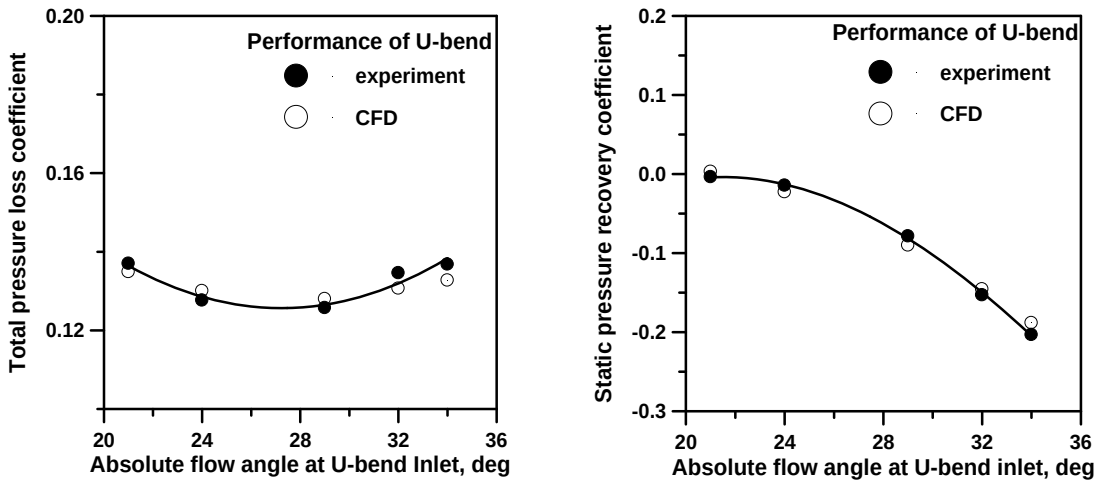

Fig. 13 Comparison of experimental and numerical data for U-bend (*RCV2*)

8. Conclusions

The flow through the stationary components of a centrifugal compressor stage is influenced by the flow angle at 180^0 U-bend inlet and is complex in nature due to the flow separation on the return channel vane surface coupled with secondary flows across the flow path. The total pressure loss coefficient is observed to be minimum at about a U-bend inlet flow angle of 23^0 for *RCV1* and is increasing with the increase in the absolute flow angle. The loss behaviour of *RCV1* is observed to be better than *RCV2* over the tested U-bend inlet flow angle range. The static pressure recovery is found to be better at lower flow angles and there is no recovery beyond 30^0 for the chosen configurations.

A CFD study was conducted, simulating the same flow conditions of the experiment using FLUENT for *RCV2* configuration. The flow separation on the suction side of the vane and the development of secondary flows were visualised by contour and vector plots. A qualitative agreement has been observed between the experimentally measured and numerically calculated values of performance parameters for the chosen configurations. The flow separation near the leading edge of *RCV2* configuration appears to be responsible for the increased losses.

Acknowledgements

The authors acknowledge the contributions from the staff of Turbomachinery Laboratory of Corporate R&D division, BHEL during the experimental work. Acknowledgements are also due to the management of Bharat Heavy Electricals Limited for according approval to publish the work.

Nomenclature

b	flow path width, mm	p	pressure
b^*	non-dimensional flow path width (b/K)	*RCV1*	return channel vane *1*
C	velocity, m/sec	*RCV2*	return channel vane *2*
C_m^*	non-dimensional meridional velocity $(C_m)/(C_{m1})_{avg}$	r	Radius
C_p	static pressure recovery coefficient $[(p_s - p_{s1}) / (p_{t1}-p_{s1})]$	r^*	radius ratio (r/r_L)
C_{pv}	vane surface pressure coefficient $[(p_{sv} - p_{s1}) / (p_{t1}-p_{s1})]$	*T.E*	trailing edge
K	geometrical constant	α	absolute flow angle
L.E	leading edge	ζ	total pressure loss coefficient $[(p_{t1} - p_t)/ (p_{t1}-p_{s1})]$

Subscripts

avg	average	*t*	total
L	leading edge of return channel vane	*1*	U-bend inlet
m	meridional	*2*	U-bend exit
s	static	*3*	return channel vane exit
sv	static condition on return channel vane surface	*4*	90^0 bend exit

References

[1] Simon, H., and Rothstein, E., 1983, "On the Development of Return Passages of Multistage Centrifugal Compressors," ASME Fluids Engineering Division, Vol. 3, Return Passages of Multistage Turbo machinery, pp. 1-11.

[2] Inoue, Y., and Koizumi, T., 1983, "Experimental Study on Flow Patterns and Losses in Return Passages for Centrifugal Compressor," ASME Fluids Engineering Division, Vol. 3, Return Passages of Multistage Turbo machinery, pp. 13-21.

[3] Lenke, L.J., and Simon, H., 2000, Aerodynamic Analysis of Return Channels of Multi-Stage Centrifugal Compressors," ASME PID-Vol. 5, Challenges and Goals in Industrial and Pipeline Compressors, pp. 117-126

[4] Arpad Veress., and Vanden Braembussche, R., 2004, "Inverse Design and Optimization of a Return Channel for a Multistage Centrifugal Compressor," ASME Journal of Fluids Engineering, Vol. 126, pp. 799-806.

[5] Oh, J M., Engeda, A., and Chung, M K., 2005, "A Numerical Study of the U-turn Bend in Return Channel Systems for Multistage Centrifugal Compressors," Proc. I Mech E Vol. 219, part C: J. Mechanical Engineering Science, pp. 749-756.

[6] Tomitaro Toyokura and Toshiaki Kanemoto and Moriaki Hatta, September 1986, "Studies on Circular cascades for Return Channels of Centrifugal Turbomachinery" 1st report-Inverse Method and Cascade Design, Bulletin of JSME, Vol. 29, No. 255, paper: 255-22.

[7] Tomitaro Toyokura and Toshiaki Kanemoto, September 1986, "Studies on Circular cascades for Return Channels of Centrifugal Turbomachinery" 2nd report-Flows and Performances of Cascades, Bulletin of JSME, Vol. 29, No. 255, paper: 255-23.

[8] T Ch Siva Reddy, GV Ramana Murty, MVSSSM Prasad, DN Reddy, "Theoretical and Experimental Studies on Low Solidity Vaned Diffusers of a Centrifugal Compressor Stage", Proc. Of 30th National Conference on Fluid Mechanics and Fluid Power, December 11-13, 2003, NIT, Surathkal, India, pp. 621-628.

[9] James M Sorokes, Bradley R Hutchinson, "The Practical Applications of CFD in the Design of Industrial Centrifugal Compressors", ASME PID-Vol. 5, Challenges and Goals in Industrial and Pipeline Compressors, pp. 47-54.